

# CLASSIFICATION OF DIGITAL IMAGES USING FUSION ELEVATED ORDER CLASSIFIER IN WAVELET NEURAL NETWORK

<sup>1</sup>Arulmurugan, R. and <sup>2</sup>P. Sengottuvelan

Bannari Amman Institute of Technology, Sathyamangalam, TamilNadu, India

Received 2014-03-13; Revised 2014-04-21; Accepted 2014-04-26

## ABSTRACT

The revival of wavelet neural networks obtained an extensive use in digital image processing. The shape representation, classification and detection play a very important role in the image analysis. Boosted Greedy Sparse Linear Discriminate Analysis (BGS LDA) trains the cascade level of detection in an efficient manner. With the application of reweighting concept and deployment of class-reparability criterion, lesser search was made on more efficient weak classifiers. At the same time, Multi-Scale Histogram of Oriented Gradients (MS-HOG) method removes the confined portions of images. MS-HOG algorithm includes the advanced recognition scenarios such as rotations transportations on multiple objects but does not perform effective feature classification. To overcome the drawbacks in classification of higher order units, Fusion Elevated Order Classifier (FEOC) method is introduced. FEOC contains a different fusion of high order units to deal with diverse datasets by making changes in the order of units with parametric considerations. FEOC uses a prominent value of input neurons for better fitting properties resulting in a higher level of learning parameters (i.e.,) weights. FEOC method features are reduced using feature subset collection method. However, elevation mechanisms are significantly applied to the neuron, neuron activation function type and finally in the higher order types of neural network with the functions of adaptive in nature. FEOC have evaluated sigma-pi network representing both the Elevated order Processing Unit (EPU) and pi-sigma network. The experimental performance of Fusion Elevated Order Classifier in the wavelet neural network is evaluated against BGS LDA and MS-HOG using Statlog (Landsat Satellite) Data Set from UCI repository. FEOC performed in MATLAB with factors such as classification accuracy rate, false positive error, computational cost, memory consumption, response time and higher order classifier rate.

**Keywords:** Local Features, Sigma-pi Network, Fusion Elevated Order Classifier, Adaptive Functions, Wavelet Neural Network, Learning Parameters, Elevated Order Processing Unit

## 1. INTRODUCTION

The theory of wavelets is useful in recognizing the common properties for approximation for Wavelet Neural Networks (WNN) and initialization for heuristics for rapid training. WNN offer high-quality cooperation between the hi-fi implementations due to the nature of redundancy of non-orthogonal wavelet neural systems and many useful representations that are

designed using the two important properties of wavelets namely, time and frequency. Much research has been prepared on applications of WNN, which combine the capability of artificial neural networks. WNN merges the learning process and the capability of wavelet decomposition for recognition and control of dynamic systems. WNN also called Artificial Neural Networks (ANN) in (Ramírez-Quintana *et al.*, 2012) is useful for decades applied to several different fields, such as

**Corresponding Author:** Arulmurugan, R., Bannari Amman Institute of Technology, Sathyamangalam, TamilNadu, India, Tel: +919629594687

science, engineering, industry, security and medicine. Cortex-based ANN models are illustrated to end with and discuss about the throughout.

Another form of neural network, Convolutional Neural Networks (CNN) is trained to perform dynamic state features in (Shruthi, 2011). The dynamic state processes are educated using motion tracking where distance alter and particle filtering is integrated. With the distract of the similar object class, CNN does not provide mechanisms for full and long-term occlusions. Branch-and-Bound Model Selection as expressed in (Thakoor *et al.*, 2010) provides segmentation in robust manner but in a way highly dependent on the initial hypothesis level selected in wavelet form. The various available guided sampling approaches such as classification scheme are not evaluated to identify and provide with the solution space.

Wavelet-based classification scheme as described in (Hong and Liang-Zheng, 2008) extracted unique multi-scale feature of the boundary points in WNN. WNN sporadically provided comprehensive evaluation but failed to concentrate on recognizing of objects WNN. Feature selection as demonstrated in (Alexander and Vladimir, 2012) analyzed the relationship of scores obtained in the initial learning process for classifying of objects using neural network classifiers. Network classifier reduces the feature value by conserving comparable recognition potential while increasing the computational evaluations but not effective in classifier recognition capabilities. Automatic aircraft target recognition by ISAR image processing as explained in (Benedetto *et al.*, 2012) fails in applying suitable optimization algorithms to the NN learning process. Indeed, possible to operate multivariate function decomposition but fails to perform the web based learning optimization problem.

A series of object based on the web and recognition of face as demonstrated in (Laura *et al.*, 2010) tests the series of objects resulting in memory impairments while recognizing the object but impairments during the recognition of faces. Performance is impaired using visual memory being detected in six of the visual categories of dissimilar form. Rank ordering knowledge and spectro-temporal data spike-time learning mechanisms were used during on-line learning and during the recognition of spatio and spectro-temporal data (SDSP) as illustrated in (Nikola *et al.*, 2013). The SDSP learning mechanism is used to develop the network changes being observed in connection weights that extracts the spatio-temporal spike data clusters during both the levels of training and recall. An expert

system called the generalized regression neural network was presented (Mahesh *et al.*, 2014) for the diagnosis of hepatitis B virus related diseases.

The wavelet space is significantly used for object recognition whereas the signal extraction is derived using the sum being weighted sum for their interior products collectively obtained from the wavelet and signal vector. As the wavelet space combines the function of both the time frequency wavelet transform and self-studying the structure of neural networks, the network significantly achieves the robustness.

Wavelet transforms have been used as a means of denoting function in a way that highly reveals the properties of the joint time frequency space. Cortical area V2 as illustrated in (Stephen *et al.*, 2011) computes the relative disparity which is the difference of complete disparity on two visible features. With the relative unconditional nature, the disparity is highly observable under both the changes observed in the scene and the movements being observed in the eye. With the introduction of neural network, which predict the inhibition of disparity-sensitive 4 layer cell. The cells from V1 transform unconditional disparity to V2 source transform in an unconditional manner.

The problems related to the smallest level of dimension cannot be addressed for the applications related to the WNN. This is because of the reason that they are gathered using a repeated form of dilated and translated wavelets. Moreover, the wavelets increase drastically in the WNN with the dimensions. Features are extracted using Support Region (SR) as explained in (Yun-Fu *et al.*, 2011) where the LMS-trained filters are relabeled with the order of significance. Furthermore, the probability of black pixel occurrence is not considered as features. The probability of black pixel occurrence is employed as the single feature. More effective features classification is not explored to further improve image quality.

Image classification from a database is chiefly complicated for traditional machine learning algorithms since the high number of images and many details that explain an image. For these motivation, conventional machine is unstable to classify images from a database. Additionally, these machines take a long time for classification. Existing image storing systems limit classification mechanism to explain an image based on the information, quality, or shape features on WNN. One of the existing methods for recognition, classification and retrieval of images is based on WNN. Thus, because of the many images that are classified

and high number of input unit of WNN, Learning of the WNN is very difficult. Classification analysis as described in (Hassan *et al.*, 2010) evolved ensembles to incorporate Back Propagation Neural Network for the classification of datasets.

The process of pre-segmentation was not performed during the spatiotemporal localization and classification in (Antonios *et al.*, 2011). Moreover with the training being performed, the positional values of the spatial codeword were combined with the set of reference points. Additionally, the temporal positions were also obtained during the start and end level of action instance. But during the stage of testing, whenever the codeword were triggered the spatiotemporal position expands with the action, with the help of the information stored during the training phase. An illustration of the object using two methods namely sparse coding and multi-scale max pooling as demonstrated in (Qing *et al.*, 2012) represent, a linear classifier to distinguish the target from the background and account for the target and backdrop exterior variations over time. The non-orthogonal, over-complete dictionary learned from local patches construct visual prior more effectual for object description.

To handle high dimensionality objects, image classification regularly relies on a preprocessing step to reduce the information of images. The reduced set is then used as new input variables of WNN. One of the preprocessing phases is based on wavelet neural transform. Wavelet neural transforms at the moment in the mainly accepted method to analyze images and present information from an image such as a shape and texture.

In this study, Fusion Elevated Order Classifier (FEOC) method reduces the feature set by using feature subset collection method. The FEOC wavelet neural network takes the original input for the simplest structure construction. On the other hand, elevation concept is widely developed in FEOC neuron type with adaptive functions. FEOC employs input neurons with a higher level of correlation for fixing the properties in a better manner resulting in the increasing value of parameters being learned (i.e.) varying weights. Many efforts are taken to decrease the false positive error for efficient result. FEOC have been considered sigma-pi network (i.e.) EPU and pi-sigma network for higher order classifier rate.

The structure of the paper is as follows. In Section 1, describe the wavelet neural network and image classification disadvantages in WNN. In section 2, demonstrates the Fusion Elevated Order Classifier method to deal with higher order units and fusion

concept. Section 3 explains about the dataset from UCI repository with parametric factor description. Section 4 performs result analyzation using table and graph. Section 5 illustrates the related work and finally concluded the work in section 6.

## 2. FUSION ELEVATED ORDER CLASSIFIER ON WAVELET NEURAL NETWORK

Fusion Elevated Order Classifier uses the fusion concept to deal with Landsat Satellite dataset by updating the orders of differing units and changing the parameters accordingly. Landsat Satellite digital images were extracted by decomposing the input image using even wavelet neural transformation. Therefore Fusion Elevated Order Classifier (FEOC) method is illustrated in diagrammatic form in **Fig 1**.

Fusion elevated order classifier takes landsat satellite digital images from the UCI repository dataset as the input for the simple construction. The critical work to be performed in wavelet neural network transformation is to differentiate any random function for a superposition set of such wavelets. The common functionalities in FEOC method are achieved using single wavelet prototype called as even wavelet followed by the operations of scaling and translation operations. At the same time, the FEOC method when compared to the conventional Fourier methods, the FEOR provides better results during analyzing the situations with signal consisting of discontinuities and sharp spikes.

Initially, FEOC, wavelet neural network transformation preprocessed by converting an RGB image into a Gray Scale image. An RGB (Red, Blue and Green) image is an array of pixels and the number of bits used to match up to a pixel value determines the bit depth of an RGB image. The RGB images are transformed into Gray Scale images for easier processing of satellite images. The even Wavelet neural Transform (WT) for feature extraction in FEOC provides a time frequency representation of the signal. Wavelet transforms with feature subset collection are used to reduce the number of bits required to represent an image. Feature reduction is done in order to get useful information from the images. A transform is done by applying even wavelet transformation. The gray scaled image undergoes wavelet neural decomposition and the satellite image is decomposed using even wavelets to reduce the features.

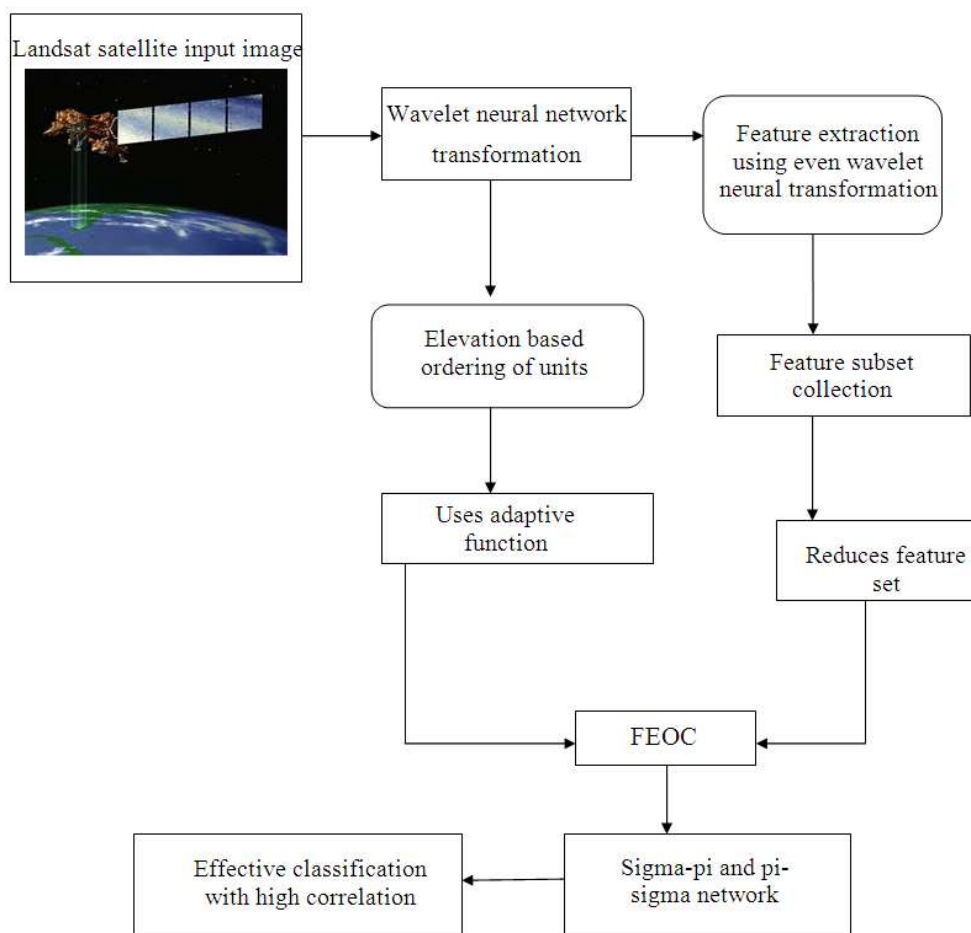


**Fig. 1.** Architecture diagram of FEOC method

Elevation based ordering of units contains various higher order units in FEOC method. The order of each elevated order unit dynamically changes its training process (i.e.,) decrease and increase to obtain a desired accuracy using adaptive functions. Adaptive function in FEOC focuses on making the light coefficient of the same features, so that the classifier design is directly adopted. The classifier design of FEOC fuses the reduced feature set and adaptive function on Sigma-pi and pi-sigma network to achieve effective classification with high correlation.

### 2.1. Preliminaries for Feature Extraction

Assume the general sigma-pi model in FEOC for ‘N’ (first order, second order and third order up to ‘N’ order) structures include two features, such as  $x_1$  and  $x_2$  in every sample. To perform classification, FEOC extracts

textual features based on grey color. The extracted features are further estimated using a second order representation of grey satellite images. Furthermore, FEOC considers the co-occurrence matrices for statistical model encoded within the portion of sub-images. With the second order representation of grey satellite images, FEOC confines towards grey level information which are highly significant towards the discrimination of textures.

Based on the types of features, the values of the texture are either placed nearer or scattered. For textures of coarse property, the covariance matrices have higher values than for fine textures where their values are scattered. Moreover, the co-occurrence matrices encode the level of wavelet based on the second order estimation of probability density function. Probability density function  $p(a,b,d,\infty)$  is

calculated by including all pairs of pixels at distance 'd' have wavelet neural coefficients of intensity 'a' and 'b', at a particular direction '∞'. The angular displacement used is the FEOC set {0, π/4, π/2 and 3π/4} which gives a measure of correlation, directional linearity, inverse difference moment and entropy defined respectively Equation 1 and 2:

$$X_1 = \sum_{a=1}^N \sum_{b=1}^N f(a,b)^2 \tag{1}$$

$$X_2 = \frac{\sum_{a=1}^N \sum_{b=1}^N (a,b)f(a,b) - \mu_a \mu_b}{\sigma_a \sigma_b} \tag{2}$$

where, f(a,b) is the a,b entry of normalized co-occurrence matrix, N the number of levels in the wavelet network and μ<sub>a</sub>, μ<sub>b</sub>, σ<sub>a</sub>, σ<sub>b</sub> are the means and standard deviations of the marginal probability by summing up the rows of the matrix f(a,b). The original satellite image 'S' transforms the color into three channel levels as denoted below Equation 3:

$$S_i; i = 1, 2, 3 \tag{3}$$

where, 'i' stands for decomposed channel set. A three level even wavelet neural frame transformation is applied to each channel S<sub>i</sub> in FEOC to reduce the feature set. The transformation results in a new representation of the original image by a low resolution image and the feature images. Therefore the new representation is defined as Equation 4:

$$S_i = M\{M_n^i, E_m^i\} \tag{4}$$

The information of the texture is presented for 'n' decomposition level for even wavelet channels followed by the subsequent level of the coefficients are measured. Therefore the new representation comprises of satellite images for values m = 4, 5, 6, ..., n with i = 1, 2 and 3. Similarly, the second order texture information is obtained from the co-occurrence matrices for different sub satellite images. These resultant co-occurrence matrices confine spatial interrelations between the intensity levels surrounded by level of wavelet decomposition of even order. Finally, the resultant co-occurrence matrices obtained in FEOC produces four varied directions with different resultant matrices.

**2.2. Elevation Ordering of Units in Neural Network**

The better fitting properties in FEOC obtain higher correlation by updating the difficult parameter. Elevated

order of neural classifier initial layer which includes online updating orders with Polynomial Elevated Order Neural Networks (PEONN), Trigonometric Elevated Order Neural Networks (TEONN), Sigmoid Polynomial Elevated Order Neural Networks (SPEONN). PEONN chooses the adaptive function as a polynomial function. Accordingly, in FEOC method neuron activation function, p(x) is even.

In TEONN the adaptive functions are of trigonometric pattern of sine and cosine values. Cosine and sine alternately used over the features. For e.g., for Landsat satellite data set including two features as Equation 5:

$$\left. \begin{aligned} p(x1) &= \cos(x1) \\ p(x2) &= \sin(x2) \end{aligned} \right\} \tag{5}$$

In SPEONN the adaptation functions are SIGMOID functions. Both LOGSIGN and TANSIGN functions are used in FEOC:

$$p(x) = \frac{1 - e^{-x}}{1 + e^{-x}} \tag{6}$$

$$p(x) = \frac{1}{1 + e^{-x}} \tag{7}$$

where, Equation 6 represents the LOGSIGN and Equation 7 represents the TANSIGN. In second layer, even combinations of wavelet neural units are chosen. FEOC fuses the entire elevated order neural network together to obtain the higher correlation classification process. Even combination of the units is grouped together in second elevated layer including neuron type and neuron activation function type.

Figure 2 shows a general aspect of fusion in elevated order units. Generally, FEOC comprises of different units of high-order. During the training process, the ordering of the high-order unit changes in a dynamic manner in order to obtain the classifier accuracy of desired level for validating the samples containing digital images. As illustrated in Fig. 2, the output consists of an adaptive function which identifies different classes for testing the binary coding with bit values (0, 1). FEOC output 'Q' during the test process is shown in Sigma-pi and pi-sigma network as:

$$Q = I * W \tag{8}$$

$$W = W_{b0} + \sum_{b=1}^k W_{b1} I_b(x1, x2) \tag{9}$$

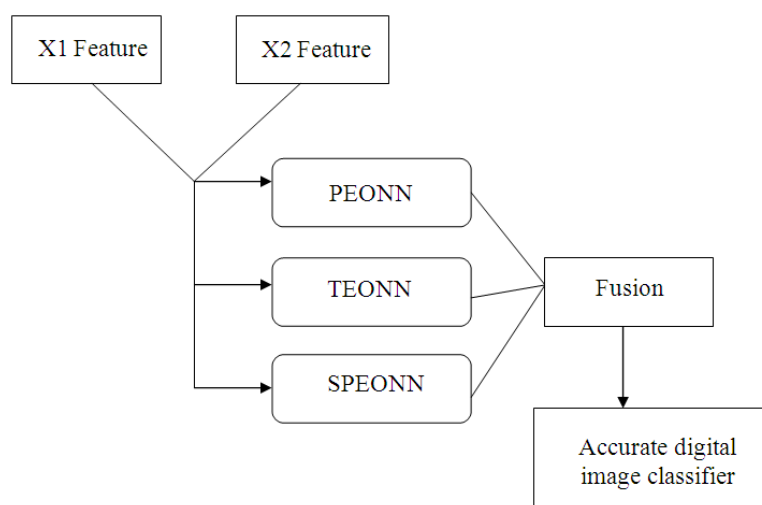


**Fig. 2.** Fusion of elevation order units

Equation 8 denote ‘I’ as the input values and ‘W’ weight matrix of second elevated layer. K represents value of order greater than 0 whereas denotes the digital image features. The normalized weight for co-occurrence matrices are represented by  $W_{b0}$ ,  $W_{b1}$ .

### 2.3. Fusion Elevated Order Classifier Algorithm

Wavelet neural network develops the fusion elevated order classifier with adaptive function. FEOC algorithm is described as:

// Fusion Elevated Order Classifier

Start

Step 1: Input digital image represents the input vector

Step2: Performs the wavelet transformation preprocessing step

2.1: Convert RGB value to gray value

Step 3: Feature Extraction with given Input vector

3.1: Feature subset collects angular displacement ratio

3.2: Reduces the feature set using means and standard deviations computation by marginal probability

Step 4: Elevation based ordering of units

4.1: Adaptive function of PEONN, SPEONN, TEONN

4.2: Interface region combines the signal from the input region through weights value in

Sigma-pi and pi-sigma network

4.3: Fusion of Elevated order units for high correlation

4.4: Weight updated using Equation (8) and (9) computation on Validation digital image samples.

Step 5: Output digital image reached to the desired binary bit code with effective classification

End

In essence, the wavelet neural network operates by summing the outputs from all elevated order units. Elevated units serve to classify the input digital images into classes with lesser number of feature set. FEOC behavior is useful in classification applications, where estimate the likelihood of any predefined attribute classes in dataset. The order of elevated units specifies the neuron values in the initial layer whereas FEOC’s second layer is of the form even order. Experiments conducted also revealed that the accuracy obtained to be of optimum level if the values of neurons selected is same as that of the bits obtained as output.

### 3. SIMULATOR DESCRIPTION WITH PARAMETRIC FACTORS

Fusion Elevated Order Classifier (FEOC) method on wavelet neural network is experimented on MATLAB code. FEOC method uses Statlog (Landsat Satellite) Data Set with multi-spectral values. The multi-spectral values for FEOC method is extracted for the pixels ranging  $3 \times 3$  for the satellite image and classification of images is performed with pixel lying in the centre of each neighborhood. With the given multi-spectral values, FEOC predicts accurate classification with test database and the pixel is denoted in the form of the integer and lies between 0 and 255.

The Landsat satellite using for simulating FEOC method is a great source of information extractable for a

scene. The interpretation of a scene is then integrated with the spatial data comprising of different types and various resolutions that includes both the multi-spectral and radar data. This largely indicates the topography with the landforms of significant importance characterized by aggregated approaches for remote sensing. The existing methods are not well equipped for different types of data. On the other hand, the FEOC method using the integer values ranging from 0 to 255 and single resolution provides maximum-likelihood classification performs very well.

A single frame of Landsat MSS imagery used in FEOC method comprises of four digital images of similar scene for differing spectral bands. Out of the four digital images, two images are present in the visible region whereas the other two are nearer to the infra-red. Each pixel in FEOC method comprises of 8-bit binary word, where 0 denotes black whereas 255 represents white with spatial resolution for each pixel about 80×80 m with each image consisting of 2340×3380 such pixels. The data corresponds to a 3\*3 square neighborhood of pixels with four spectral bands in 3 \*3 3 neighborhood with each integer values denoted for each classes. Along with the data, the four spectral values are provided and then the pixels are read from left-to-right and top-to-bottom. Accordingly, interested in assess the performance of FEOC method against existing BGS LDA mechanism and MS-HOG method.

#### 4. RESULT ANALYSIS OF LCSAD FRAMEWORK

Fusion Elevated Order Classifier (FEOC) method is compared against the existing Boosted Greedy Sparse Linear Discriminate Analysis (BGS LDA) and Multi-scale Histogram of Oriented Gradients (MS-HOG) method. Classification accuracy parameter in FEOC indicates the extent to which it is able to accurately classify digital images with lesser features, measured in terms of percentage (%). False positive error occurs when the statistical analysis of a trial detects a difference in outcomes between an input group image and a control group image in FEOC method against existing system:

$$\text{False positive error} = \frac{\text{False positive value}}{\text{False positive value} + \text{True positive value}}$$

Computational cost is term as the theory of amount consumes to perform the FEOC operation. A computational cost problem is solved in FEOC and it is measured in terms of milliseconds (ms). Memory

consumption factor is also measured in FEOC, describe as the amount of memory consumed while experiment the digital images. The digital image is stored after the classifier operation in database, measured in terms of Kilo Bytes (KB). Response time factor is measured as the amount of time taken to perform simple operations on satellite images after the input request.

The FEOC response time is also compared with the existing BGS LDA and MS-HOG method, measured in terms of seconds (sec). Higher order classifier is the rate at which the effective classification performed in wavelet neural network system. Classifier rate fuses the higher order of system such as PEONN, TEONN and SPEONN to achieve higher percentage value in FEOC method. The below evaluation value through **Table 1** and graph describes the FEOC method improvements with beneficial experimental results when compared with existing system.

The classification accuracy rate is measured based on the boosting rounds in BGS LDA, MS-HOG method and FEOC method (**Fig. 3**). FEOC behavior is useful in classification applications in estimating the likelihood of any predefined attribute classes in Landsat Satellite dataset. The number of neurons in initial layer is directly specified by the order of elevated units in an even order and experiments reveal that the desired classification accuracy is reached. The classification accuracy is 8-12% in FEOC method when compared with the BGS LDA model (Chunhua *et al.*, 2011) and 4-7% improved when compared with the MS-HOG method (Yuhua *et al.*, 2011).

**Table 2** demonstrates the false positive error based on the features in dataset. Feature are taken in the form of 6, 12, 18, 24 upto 42 for conducting the experiment with Landsat Satellite dataset. False positive error is measured in terms of pixel count which removes the error occurrence in FEOC method.

**Figure 4** describes the false positive error rate in FEOC method. False positive error o FEOC is reduced to 18-23% when contrast against the BGS LDA Model (Chunhua *et al.*, 2011) and 5-11% reduced when compared with the MS-HOG method (Yuhua *et al.*, 2011). False positive error reduces gradually in the FEOC by applying even wavelet neural transform for feature extraction. Features in FEOC provide a time frequency representation of the signal. Signal representation in wavelet transforms reduces the number of false positive error in digital image.

**Table 3 and Fig. 5** illustrate the computational cost based on the weight count, which is measured in terms of milliseconds (ms). The weight count measures the cost taken to perform the operations in

FEOC and existing methods on using the Landsat Satellite dataset digital images. For the extraction of the second order statistical textural information co-occurrence matrices is used over the dissimilar sub satellite images. The co-occurrences of matrixes in FEOC reduces the computational cost by 7-10% when compared with the BGS LDA Model (Chunhua *et al.*, 2011) and 2-8% reduced when compared with MS-HOG method (Yuhua *et al.*, 2011).

**Table 4 and Figure 6** describes the memory consumption based on the digital image size in BGS LDA Model, MS-HOG method and FEOC method. The Size of digital image and memory consumption is measured in terms of Kilo Bytes (KB). For FEOC method, matrixes tend to have higher values near the main diagonal, whereas lower texture values are scattered. The co-occurrence matrixes encode the wavelet level for light dependence based on the estimation of the second order mutual restricted probability density function, so that memory consumption level is reduced. When compared with BGS LDA Model (Chunhua *et al.*, 2011), memory consumption is 8-12% reduced in FEOC method and also when compared with MS-HOG method (Yuhua *et al.*, 2011) 1-5% the memory level is reduced.

**Table 1.** Tabulation for classification accuracy rate

| No. of boosting rounds | Classification accuracy rate (%) |               |             |
|------------------------|----------------------------------|---------------|-------------|
|                        | BGS LDA Model                    | MS-HOG method | FEOC method |
| 5                      | 77                               | 83            | 87          |
| 10                     | 69                               | 70            | 75          |
| 15                     | 74                               | 76            | 80          |
| 20                     | 63                               | 65            | 70          |
| 25                     | 78                               | 82            | 86          |
| 30                     | 74                               | 78            | 83          |
| 35                     | 82                               | 88            | 92          |

**Table 2.** False positive error tabulation

| No. of features | False positive error (pixel count) |               |             |
|-----------------|------------------------------------|---------------|-------------|
|                 | BGS LDA model                      | MS-HOG method | FEOC method |
| 6               | 165                                | 149           | 134         |
| 12              | 310                                | 249           | 237         |
| 18              | 525                                | 452           | 412         |
| 24              | 383                                | 327           | 294         |
| 30              | 433                                | 373           | 335         |
| 36              | 274                                | 233           | 214         |
| 42              | 721                                | 615           | 564         |

**Table 3.** Tabulation of computational cost

| Weight count (KB) | Computational cost (ms) |               |             |
|-------------------|-------------------------|---------------|-------------|
|                   | BGS LDA model           | MS-HOG method | FEOC method |
| 15                | 2529                    | 2438          | 2324        |
| 30                | 2543                    | 2449          | 2336        |
| 45                | 2555                    | 2468          | 2349        |
| 60                | 2651                    | 2564          | 2440        |
| 75                | 2674                    | 2688          | 2466        |
| 90                | 2709                    | 2582          | 2499        |
| 105               | 2839                    | 2598          | 2534        |

**Table 4.** Tabulation of memory consumption

| Size of image (KB) | Memory consumption (KB) |               |             |
|--------------------|-------------------------|---------------|-------------|
|                    | BGS LDA model           | MS-HOG method | FEOC method |
| 75                 | 1423                    | 1345          | 1292        |
| 150                | 1654                    | 1504          | 1452        |
| 225                | 1941                    | 1810          | 1785        |
| 300                | 2310                    | 2238          | 2126        |
| 375                | 2771                    | 2656          | 2553        |
| 450                | 3189                    | 3080          | 2928        |
| 525                | 3545                    | 3340          | 3245        |

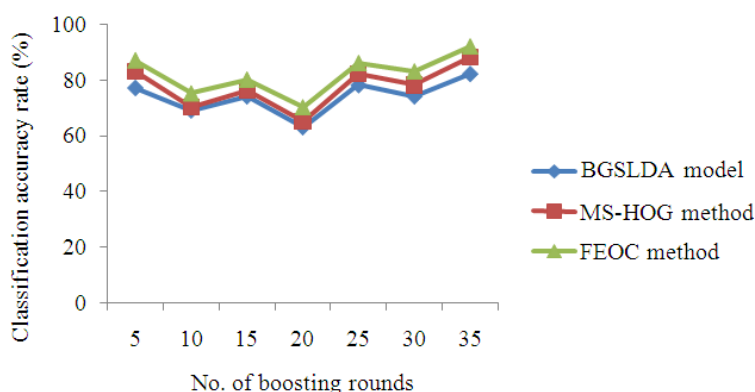


**Fig. 3.** Classification accuracy rate measure



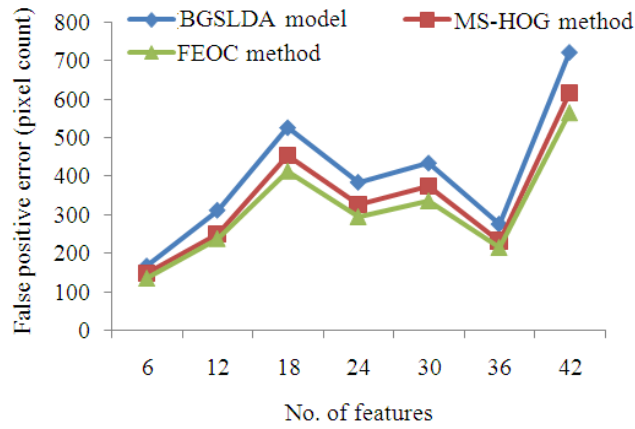


Fig. 4. False positive error measure

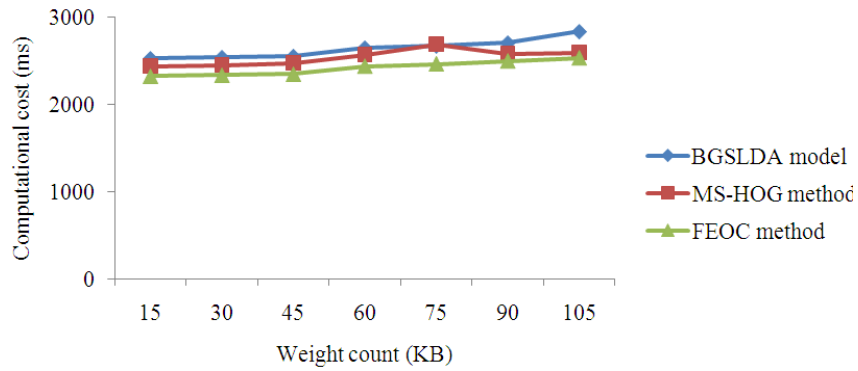


Fig. 5. Performance of computational cost

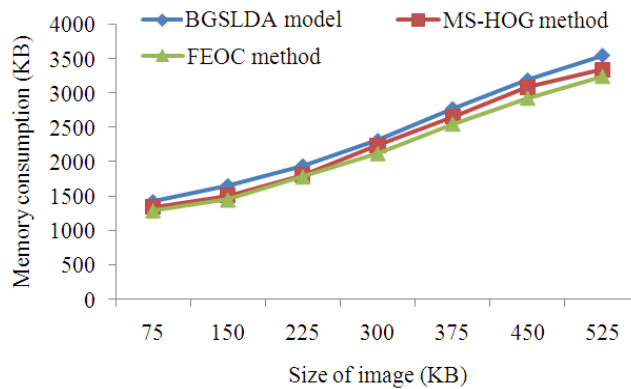


Fig. 6. Measure of memory consumption

Table 5 and Figure 7 depicts the response time based on the frame number. The experiments conducted on the 20, 40, 60, 80, 100, 120, 140, 160th frame number to compute the response time. The FEOC output 'Q' in

Sigma-pi and pi-sigma network takes the weight matrix of second elevated layer. Equation 8 and 9 compute response time of digital images and reduces up to 14-17% of repose time in FEOC when compared with the BGS LDA Model

(Chunhua *et al.*, 2011) and 4-6% reduced when compared with the MS-HOG method (Yuhua *et al.*, 2011).

**Table 6 and Figure 8** illustrates the higher order classifier rate based on the class number. The class number in **Fig. 8** denotes the classes in Landsat Satellite Data Set. FEOC fuses entire elevated order neural network together to obtain the higher correlation classification process. Even combination of the units is grouped together in second elevated layer including neuron type and neuron activation function type to achieve higher classifier rate. The classifier rate is improved by 9-12% in FEOC when compared with the BGSLDA Model (Chunhua *et al.*, 2011) and 3-5% improved when compared with the MS-HOG method (Yuhua *et al.*, 2011).

Finally, FEOC method achieves the higher correlation ratio with effective classification. Based on diverse confined pixel information, appropriate digital images are easily taken as input parameter to perform the FEOC operations. Each of these figures with overall parametric result shows the good accuracy rate and also very useful method for diminishing the response time on relatively Landsat Satellite Data Set from UCI repository.

**Table 5.** Tabulation for response time measure

| Frame number | Response time (sec) |               |             |
|--------------|---------------------|---------------|-------------|
|              | BGSLDA model        | MS-HOG method | FEOC method |
| 20           | 720                 | 647           | 615         |
| 40           | 655                 | 579           | 552         |
| 60           | 868                 | 773           | 724         |
| 80           | 592                 | 512           | 491         |
| 100          | 622                 | 551           | 514         |
| 120          | 451                 | 399           | 374         |
| 140          | 647                 | 578           | 538         |
| 160          | 868                 | 785           | 742         |

**Table 6.** Tabulation of higher order classifier rate

| Neuron class number | Higher order classifier rate (%) |               |             |
|---------------------|----------------------------------|---------------|-------------|
|                     | BGSLDA Model                     | MS-HOG method | FEOC method |
| 1                   | 83                               | 88            | 91          |
| 2                   | 84                               | 90            | 93          |
| 3                   | 85                               | 91            | 95          |
| 4                   | 78                               | 82            | 86          |
| 5                   | 79                               | 84            | 87          |
| 6                   | 82                               | 87            | 92          |
| 7                   | 84                               | 88            | 93          |

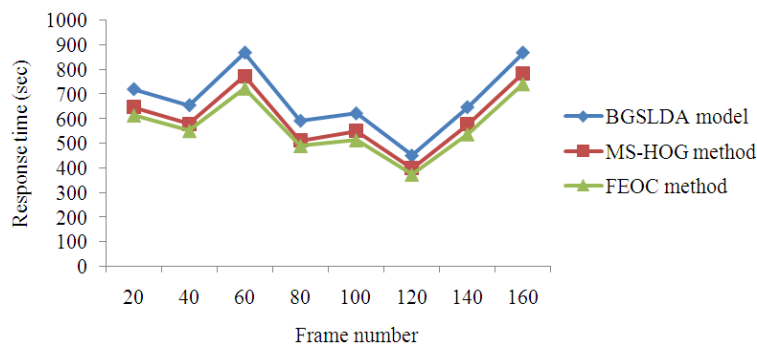


**Fig. 7.** Measure of response time

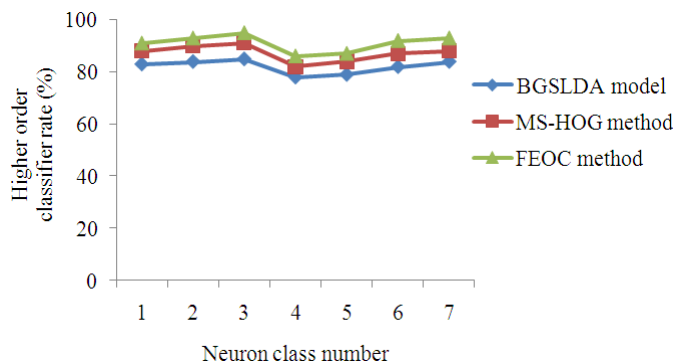


**Fig. 8.** Measure of higher order classifier rate

## 5. RELATED WORK

The wavelet neural networks combine the utility function of the time frequency localization from wavelet transform and self-study the structure of neural network. Multi-Scale Histograms of Oriented Gradients (MS-HOG) method as described in (Yuhua *et al.*, 201) extract features of local values from images in the form of visual objects. The model has multiple layers but contains only one input and output layer. MS-HOG does not include the rotation, transportations on multiple objects.

Quality assessment algorithm as demonstrated in (Alexandre *et al.*, 2011) for blurred images combine the diverse metrics in a classifier with the neural network structure. The majority of the analyzed metrics relay on the knowledge of the digital images. Boosted Greedy Sparse Linear Discriminate Analysis (BGS LDA) as shown in (Chunhua *et al.*, 2011) proficiently instructs a detection cascade. Due to this, during the process of learning, the coefficients of weak classifiers which is to be preferred frequently updates based on the values of the mentioned standards. BGS LDA using the property of boosting based on the sample reweighting and the criterion of GS LDA called the class-reparability which fails to search the classifiers of weak nature and updating the learned model online.

A pre-trained boosting-style detector as illustrated in (Junbiao *et al.*, 2011) encodes the priori information based on the features being preferred and weighting the weak classifiers. At the same time, CovBoost does not have the provisioning for handling the time-varying scenes in the online learning model. To provide solutions to these, the online updating model was integrated with the parameterized CovBoost. Boosting color-component feature selection framework as depicted in (Choi *et al.*, 2011) find the best set of color-component features from various color spaces. However, other face features fails to readily incorporate to identify the most significant features for face recognition task. They do not discover the mixture of the components of color variation with the variations observed during the illumination.

Pulse-Coupled Neural Network (PCNN) with multichannel (MPCNN) as expressed in (Hualiang *et al.*, 2012) performs color image segmentation. Different from the conventional PCNN, pulse-based radial basis function units are initiated into the model neurons of PCNN. PCNN determine the fast links among neurons with respect to their spectral feature vectors and spatial proximity but does not provide mechanisms to handle with the images comprising the spectral information.

The structured max-margin learning algorithm as presented in (Jianping *et al.*, 2011) chooses the image visual conception network. Max-margin Markov networks and multitask learning deal with huge inter concept visual resemblance of spectral information more effectively. Structured max-margin learning algorithm fails to extend parallel evaluative platforms based on cluster on visual concept network for training the classifiers based on the inter-related model. It was also not very much suitable in dealing with the nearest neighbors of range of higher for the process of classifying inter-related nature.

## 6. CONCLUSION

Fusion Elevated Order Classifier fuses all the high order units to deal with high classification accuracy rates. FEOC reduces the feature set using feature subset collection method and acts significantly with large size datasets. In summary, FEOC method concludes that the classification performed excellently over datasets with less features. FEOC uses the better fitting properties to attain high correlation ratio of features. With the help of different correlation of features, FEOC results in better accuracy even for low-feature dataset. By diminishing the number of features, the FEOC method is able to check more correlations over features. Adaptive function with elevation concept achieves the higher order fusion with neuron type, neuron activation function in sigma-pi and pi-sigma network. Theoretical analysis and experimental results show that, FEOC method attains the maximal classification accuracy rate, higher order classifier rate. Experiment on Landsat Satellite Data Set attains minimal false positive error, 4.701% reduced computational cost in FEOC with minimal memory consumption and response time.

## 7. REFERENCES

- Alexander, G. and G. Vladimir, 2012. Investigation of efficient features for image recognition by neural networks. *Neural Netw.*, 28: 15-23. DOI: 10.1016/j.neunet.2011.12.002
- Alexandre, C., A.L. da Costa, E.A. da Silva, A. Said and R. Samadani *et al.*, 2011. No-reference blur assessment of digital pictures based on multifeature classifiers. *IEEE Trans. Image Process.*, 20: 64-75. DOI: 10.1109/TIP.2010.2053549, PMID: 21172744

- Antonios, O., P. Ioannis and P. Maja, 2011. Spatiotemporal localization and categorization of human actions in unsegmented image sequences. *IEEE Trans. Image Process.*, 20: 1126-1140. DOI: 10.1109/TIP.2010.2076821
- Benedetto, F., F.R. Fulginei, A. Laudani and G. Albanese, 2012. Automatic aircraft target recognition by ISAR image processing based on neural classifier. *Int. J. Adv. Comput. Sci. Applic.*, 3: 96-103. DOI: 10.14569/IJACSA.2012.030816
- Choi, J.Y., Y.M. Ro and K.N. Plataniotis, 2011. Boosting color feature selection for color face recognition. *IEEE Trans. Image Process.*, 20: 1425-1434. DOI: 10.1109/TIP.2010.2093906
- Chunhua, S., P. Sakrapee and Z. Jian, 2011. Efficiently learning a detection cascade with sparse eigenvectors. *IEEE Trans. Image Process.*, 20: 22-25. DOI: 10.1109/TIP.2010.2055880
- Hassan, H.T., M.U. Khalid and K. Imran, 2010. Intelligent object and pattern recognition using ensembles in back propagation neural network. *Int. J. Electr. Comput. Sci.*, 10: 52-52.
- Hong, P. and X. Liang-Zheng, 2008. Efficient object recognition using boundary representation and wavelet neural network. *IEEE Trans. Neural Netw.*, 19: 2132-2149. DOI: 10.1109/TNN.2008.2006331
- Hualiang, Z., L. Kay-Soon and Y. Wei-Yun, 2012. Multichannel pulse-coupled-neural-network-based color image segmentation for object detection. *IEEE Trans. Indust. Electron.*, 59: 3299-3388. DOI: 10.1109/TIE.2011.2165451
- Jianping, F., S. Yi, Y. Chunlei and Z. Ning, 2011. Structured max-margin learning for inter-related classifier training and multilabel image annotation. *IEEE Trans. Image Process.*, 20: 837-854. DOI: 10.1109/TIP.2010.2073476
- Junbiao, P., H. Qingming, Y. Shuicheng, J. Shuqiang and Q. Lei, 2011. Transferring boosted detectors towards viewpoint and scene adaptiveness. *IEEE Trans. Image Process.*, 20: 1388-1400. DOI: 10.1109/TIP.2010.2103951
- Laura, G., C. Nathan, D. Emrah and D. Bradley, 2010. A new selective developmental deficit: Impaired object recognition with normal face recognition. *Cortex*, 47: 598-607. DOI: 10.1016/j.cortex.2010.04.009
- Mahesh, C., E. Kannan and M.S. Saravanan, 2014. Generalized regression neural network based expert system for hepatitis B diagnosis. *J. Comput. Sci.*, 10: 563-569. DOI : 10.3844/jcssp.2014.563.569
- Nikola, K., D. Kshitij, N. Nuttapod and I. Giacomo, 2013. Dynamic evolving spiking neural networks for on-line spatio- and spectro temporal pattern recognition. *Neural Netw.*, 41: 188-201. DOI: 10.1016/j.neunet.2012.11.014
- Qing, W., C. Feng, Y. Jimei, X. Wenli and Y. Ming-Hsuan, 2012. Transferring visual prior for online object tracking. *IEEE Trans. Image Process.* 21: 3296-3305. DOI: 10.1109/TIP.2012.2190085
- Ramírez-Quintana, J.A., M.I. Chacon-Murguia and J.F. Chacon-Hinojos, 2012. Artificial neural image processing applications: A survey. *Eng. Lett.*, 20: 68-80.
- Shruthi, S., 2011. Vehicle tracking using convolutional neural network. *Proceedings of the World Congress on Engineering, (WCE '01)*, pp: 69-69.
- Stephen, G., S. Karthik and Y. Arash, 2011. On the road to invariant object recognition: How cortical area V2 transforms absolute to relative disparity during 3D vision. *Neural Netw.*, 24: 686-692. DOI: 10.1016/j.neunet.2011.03.021
- Thakoor, N., J. Gao and V. Devarajan, 2010. Multibody structure-and-motion segmentation by branch-and-bound model selection. *IEEE Trans. Image Process.*, 19: 1393-1402. DOI: 10.1109/TIP.2010.2042647
- Yuhua, Z., M. Yan and J. Yaochu, 2011. Object recognition using a bio-inspired neuron model with bottom-up and top-down pathways. *Neurocomputing*, 74: 3158-3169. DOI: 10.1016/j.neucom.2011.04.020
- Yun-Fu, L., G. Jing-Ming and L. Jiann-Der, 2011. Inverse halftoning based on the Bayesian theorem. *IEEE Trans. Image Process.*, 20: 1077-1084. DOI: 10.1109/TIP.2010.2087765